Important Notice to Authors

Attached is a PDF proof of your forthcoming article in *Physical Review D*. The article accession code is DK11738.

Please note that as part of the production process, APS converts all articles, regardless of their original source, into standardized XML that in turn is used to create the PDF and online versions of the article as well as to populate third-party systems such as Portico, CrossRef, and Web of Science. We share our authors' high expectations for the fidelity of the conversion into XML and for the accuracy and appearance of the final, formatted PDF. This process works exceptionally well for the vast majority of articles; however, please check carefully all key elements of your PDF proof, particularly any equations or tables.

Figures submitted electronically as separate PostScript files containing color appear in color in the online journal. However, all figures will appear as grayscale images in the print journal unless the color figure charges have been paid in advance, in accordance with our policy for color in print (http://journals.aps.org/authors/color-figures-print). For figures that will be color online but grayscale in print, please ensure that the text and captions clearly describe the figures to readers who view the article only in grayscale.

No further publication processing will occur until we receive your response to this proof.

Specific Questions and Comments to Address for This Paper

The numbered items below correspond to numbers in the margin of the proof pages pinpointing the source of the question and/or comment. The numbers will be removed from the margins prior to publication.

Q: Please check that all references include complete titles.

1 Second proof: Please carefully confirm that all first-proof corrections were addressed and that changes were made accurately.

2 Second proof: Please confirm the paper is now ready to be published in its current form.

3 Second proof: This query was generated by an automatic reference checking system. References [4, 8] could not be located in the databases used by the system. While the references may be correct, we ask that you check them so we can provide as many links to the referenced articles as possible.

Titles in References

The editors now encourage insertion of article titles in references to journal articles and e-prints. This format is optional, but if chosen, authors should provide titles for *all* eligible references. If article titles remain missing from eligible references, the production team will remove the existing titles at final proof stage.

Funding Information

Information about an article's funding sources is now submitted to CrossRef to help you comply with current or future funding agency mandates. Please ensure that your acknowledgments include all sources of funding for your article following any requirements of your funding sources. CrossRef's FundRef registry (http://www.crossref.org/fundref/) is the definitive registry of funding agencies. Please carefully check the following funder information we have already extracted from your article and ensure its accuracy and completeness:

- No funding information identified - please confirm this is correct.

Other Items to Check

- Please note that the original manuscript has been converted to XML prior to the creation of the PDF proof, as described above. Please carefully check all key elements of the paper, particularly the equations and tabular data.
- Please check PACS numbers. More information on PACS numbers is available online at http://journals.aps.org/PACS/.
- Title: Please check; be mindful that the title may have been changed during the peer review process.
- Author list: Please make sure all authors are presented, in the appropriate order, and that all names are spelled correctly.
- Please make sure you have inserted a byline footnote containing the email address for the corresponding author, if desired. Please note that this is not inserted automatically by this journal.
- Affiliations: Please check to be sure the institution names are spelled correctly and attributed to the appropriate author(s).
- Receipt date: Please confirm accuracy.
- Acknowledgments: Please be sure to appropriately acknowledge all funding sources.
- References: Please check to ensure that titles are given as appropriate.
- Hyphenation: Please note hyphens may have been inserted in word pairs that function as adjectives when they occur before a noun, as in "x-ray diffraction," "4-mm-long gas cell," and "*R*-matrix theory." However, hyphens are deleted from word pairs when they are not used as adjectives before nouns, as in "emission by x rays," "was 4 mm in length," and "the *R* matrix is tested."
  Note also that Physical Review follows U.S. English guidelines in that hyphens are not used after prefixes or before suffixes: superresolution, quasiequilibrium, nanoprecipitates, resonancelike, clockwise.
- Please check that your figures are accurate and sized properly. Make sure all labeling is sufficiently legible. Figure quality in this proof is representative of the quality to be used in the online journal. To achieve manageable file size for online delivery, some compression and downsampling of figures may have occurred. Fine details may have become somewhat fuzzy, especially in color figures. The print journal uses files of higher resolution and therefore details may be sharper in print. Figures to be published in color online will appear in color on these proofs if viewed on a color monitor or printed on a color printer.
- ***Overall, please proofread the entire article very carefully.***

Ways to Respond

- ***Web:*** If you accessed this proof online, follow the instructions on the web page to submit corrections.
- ***Email:*** Send corrections to aps-robot@luminad.com. Include the accession code DK11738 in the subject line.
- ***Fax:*** Return this proof with corrections to +1.855.808.3897.

If You Need to Call Us

You may leave a voicemail message at +1.855.808.3897. Please reference the accession code and the first author of your article in your voicemail message. We will respond to you via email.

$\mu \to e\gamma$ in a supersymmetric radiative neutrino mass model

Raghavendra Srikanth Hundi*

Department of Physics, Indian Institute of Technology Hyderabad,
Kandi, Sangareddy—502 285, Telangana, India

(Received 21 October 2015)

We consider a supersymmetric version of the inert Higgs doublet model, whose motivation is to explain smallness of neutrino masses and existence of dark matter. In this supersymmetric model, due to the presence of discrete symmetries, neutrinos acquire masses at loop level. After computing these neutrino masses, in order to fit the neutrino oscillation data, we show that by tuning some supersymmetry-breaking soft parameters of the model, neutrino Yukawa couplings can be unsuppressed. In the above-mentioned parameter space, we compute the branching ratio of the decay $\mu \to e\gamma$. To be consistent with the current experimental upper bound on $\mathrm{Br}(\mu \to e\gamma)$, we obtain constraints on the right-handed neutrino mass of this model.

DOI: PACS numbers: 12.60.Jv, 13.35.Bv, 14.60.Ef, 14.60.Pq

I. INTRODUCTION

There are many indications for physics beyond the standard model (SM) [1]. One among them is the existence of nonzero neutrino masses [2]. Some of the indications for new physics can be successfully explained in supersymmetric models [3]. For this reason, neutrino masses have been addressed in supersymmetry. In a neutrino mass model, there is a possibility for lepton flavor violation (LFV) [4], for which there is no direct evidence. Experiments have put upper bounds on the branching ratios of these LFV processes [5–7]. Due to the Glashow-Iliopoulos-Maiani cancellation mechanism, these processes are highly suppressed in the SM and the above-mentioned upper bounds are obviously satisfied in it. However, a signal for any LFV process with an appreciable branching ratio gives a confirmation for new physics.

In this work, we study LFV processes of the form $\ell_i \to \ell_j\gamma$ in a supersymmetrized model for neutrino masses [8]. Here, $\ell_i, i = 1, 2, 3$, are charged leptons. The above-mentioned model arises after supersymmetrizing the inert Higgs doublet model [9,10]. The inert Higgs doublet model [9] offers an explanation for neutrino masses and dark matter. In this model [9], dark matter is stable due to an exact Z_2 symmetry and the neutrinos acquire masses at the one-loop level. This model has been extensively studied and some recent works on this can be seen in Ref. [11]. Supersymmetrizing this model could bring new features and this was done in Ref. [8]. In the supersymmetrization of the inert Higgs doublet model [8], the discrete symmetry is extended to $Z_2 \times Z_2'$. In this model, dark matter can be multipartite [12] due to the presence of R parity and the Z_2' symmetry. Some variations of this model were also presented in Refs. [13,14]. In the model of Ref. [8], gauge coupling unification is possible by embedding it in a supersymmetric SU(5) structure [15]. The origin of the discrete symmetry $Z_2 \times Z_2'$, which is described above, is also explained by realizing it as a residual symmetry from a U(1) gauged symmetry [16].

In this work we consider the model of Ref. [8] and present the expression for neutrino masses, which arises from two one-loop diagrams. We will demonstrate that neutrino masses are tiny in this model if either the neutrino Yukawa couplings are suppressed or some certain soft parameters of the scalar potential are fine-tuned. We consider the latter case, in which the neutrino Yukawa couplings can be $\mathcal{O}(1)$, and they can drive LFV processes such as $\mu \to e\gamma$. In our work we assume that the slepton mass matrices and the A-terms of sleptons are flavor diagonal. Hence, in our model, lepton flavor violation is happening due to nondiagonal Yukawa couplings. Under the above-mentioned scenario, we compute the branching ratio for the decays $\ell_i \to \ell_j\gamma$. Among these decays, we show that $\mu \to e\gamma$ can give stringent constraints on model parameters, especially on the right-handed neutrino mass. Early calculations on $\mu \to e\gamma$ in a lepton-number-violating supersymmetric model can be seen in Ref. [17].

In the model of Ref. [8], apart from $\mu \to e\gamma$ there can also be an LFV decay of $\mu \to 3e$. In a type-II seesaw mechanism for neutrino masses, the decay $\mu \to 3e$ can take place at tree level, due to the presence of a triplet Higgs boson. In our model [8], there are no triplet Higgses, and hence the decay $\mu \to 3e$ will take place at loop level. The current experimental upper limit on $\mathrm{Br}(\mu \to 3e)$ is 1×10^{-12} [18], which is about 2 times larger than that of $\mathrm{Br}(\mu \to e\gamma)$. So we can expect $\mathrm{Br}(\mu \to e\gamma)$ to put somewhat tighter constraints on model parameters than that due to $\mathrm{Br}(\mu \to 3e)$. Hence, in this work we focus on the computation of $\mathrm{Br}(\mu \to e\gamma)$. It may happen that $\mathrm{Br}(\mu \to 3e)$ and $\mathrm{Br}(\mu \to e\gamma)$ may put some additional constraints on model parameters, but we study these in a separate work.

*rshundi@iith.ac.in

This paper is organized as follows. In the next section, we describe the model of Ref. [8]. In Sec. III, we present the expressions for neutrino masses and branching ratios for the decays $\ell_i \to \ell_j \gamma$. In Sec. IV, we give numerical results on neutrino masses and $\mu \to e\gamma$. We conclude in Sec. V.

II. THE MODEL

The model of Ref. [8] is an extension of the minimal supersymmetric standard model (MSSM). The additional superfields of this model are as follows: (i) three right-handed neutrino fields, $\hat{N}_i$, $i = 1, 2, 3$; (ii) two electroweak doublets $\hat{\eta}_1 = (\hat{\eta}_1^0, \hat{\eta}_1^-)$, $\hat{\eta}_2 = (\hat{\eta}_2^+, \hat{\eta}_2^0)$; (iii) a singlet field $\hat{\chi}$. Under the electroweak gauge group $\mathrm{SU}(2)_L \times \mathrm{U}(1)_Y$, the charges of these additional superfields are given in Table I. The model of Ref. [8] contains the discrete symmetry $Z_2 \times Z_2'$, under which all the quark and Higgs superfields can be taken to be even. The leptons and the additional fields described above are charged nontrivially under this discrete symmetry [8]. The purpose of this symmetry is to disallow the Yukawa term $\hat{L}_i \hat{H}_u \hat{N}_j$ in the superpotential of the model, and as a result the neutrino remains massless at tree level. Here, $\hat{L}_i = (\hat{\nu}_i, \hat{\ell}_i)$, $i = 1, 2, 3$ are the lepton doublet superfields. The singlet charged lepton superfield is represented by $\hat{E}_i^c$, $i = 1, 2, 3$. We denote up- and down-type Higgs superfields as $\hat{H}_u$ and $\hat{H}_d$, respectively.

The superpotential of our model consisting of electroweak fields can be written as [8]

$$W = (Y_E)_{ij} \hat{L}_i \hat{H}_d \hat{E}_j^c + (Y_\nu)_{ij} \hat{L}_i \hat{\eta}_2 \hat{N}_j + \lambda_1 \hat{H}_d \hat{\eta}_2 \hat{\chi} + \lambda_2 \hat{H}_u \hat{\eta}_1 \hat{\chi} + \mu \hat{H}_u \hat{H}_d + \mu_\eta \hat{\eta}_2 \hat{\eta}_1 + \frac{1}{2} \mu_\chi \hat{\chi} \hat{\chi} + \frac{1}{2} M_{ij} \hat{N}_i \hat{N}_j. \quad (1)$$

Here, there is a summation over indices i, j which run from 1 to 3. The first and second terms in the above equation are Yukawa terms for charged leptons and neutrinos, respectively. But, as described before, $\hat{\eta}_2$ is odd under the discrete symmetry of the model and hence the scalar component of it does not acquire a vacuum expectation value [8]. So neutrinos are still massless at tree level. Apart from the superpotential of Eq. (1), we should consider the scalar potential. The relevant terms in the scalar potential are given below:

TABLE I. Charge assignments of additional superfields of the model under the electroweak gauge group.

Field	$\hat{N}_i$	$\hat{\eta}_1$	$\hat{\eta}_2$	$\hat{\chi}$
$\mathrm{SU}(2)_L \times \mathrm{U}(1)_Y$	(1, 0)	(2, −1/2)	(2, 1/2)	(1, 0)

$$V = (m_L^2)_{ij} \tilde{L}_i^\dagger \tilde{L}_j + m_{\eta_1}^2 \eta_1^\dagger \eta_1 + m_{\eta_2}^2 \eta_2^\dagger \eta_2 + m_\chi^2 \chi^* \chi + (m_N^2)_{ij} \tilde{N}_i^* \tilde{N}_j + \Big[(AY_\nu)_{ij} \tilde{L}_i \eta_2 \tilde{N}_j + (A\lambda)_1 H_d \eta_2 \chi + (A\lambda)_2 H_u \eta_1 \chi + b_\eta \eta_2 \eta_1 + \frac{1}{2} b_\chi \chi\chi + \frac{1}{2} (b_M)_{ij} \tilde{N}_i \tilde{N}_j + \text{c.c.} \Big]. \quad (2)$$

As we have explained before, our motivation is to study LFV processes in the above-described model. The LFV processes can be driven by charged sleptons. For instance, the off-diagonal elements of soft parameters, $(m_L^2)_{ij}$, can drive LFV processes. Similarly, we can write soft mass terms for singlet charged sleptons, $\tilde{E}_i, i = 1, 2, 3$, in the scalar potential. Also, there can exist A-terms connecting $\tilde{L}_i$ and $\tilde{E}_j$. The off-diagonal terms of the above-mentioned soft terms can drive LFV processes, which actually exist in the MSSM. Since our model [8] is an extension of the MSSM, we are interested in LFV processes generated by the additional fields of this model. Hence, we assume that the off-diagonal terms of the soft terms (which are described above) are zero.

For simplicity, we assume that the parameters of the superpotential and scalar potential of our model are real. Then, by an orthogonal transformation among the neutrino superfields $\hat{N}_i$, we can make the following parameters diagonal:

$$M_{ij} = M_i \delta_{ij}, \quad (m_N^2)_{ij} = (m_N^2)_i \delta_{ij}, \quad (b_M)_{ij} = (b_M)_i \delta_{ij}. \quad (3)$$

By going to an appropriate basis of $\hat{L}_i$ and $\hat{E}_j$, we can get the Yukawa couplings for charged leptons to be diagonal. After doing this, we are left with no freedom and hence the neutrino Yukawa couplings $(Y_\nu)_{ij}$ can be nondiagonal. These nondiagonal Yukawa couplings can drive LFV processes such as $\ell_i \to \ell_j \gamma$. These LFV processes are driven at the one-loop level, which we describe in the next section. As explained before, neutrinos also acquire masses at the one-loop level in this model [8]. To calculate these loop diagrams we need to know the mass eigenstates of the scalar and fermionic partners of the fields shown in Table I, since these fields enter into the loop processes. Expressions for these mass eigenstates are given in Ref. [19]. However, our notations and conventions are different from those of Ref. [19]. Hence, for the sake of completeness we present them below.

The charged components of $\hat{\eta}_1, \hat{\eta}_2$ can be fermionic and scalar, which can be written as $(\tilde{\eta}_1^-, \tilde{\eta}_2^+)$ and (η_1^-, η_2^+), respectively. The two charged fermions represent chargino-type fields whose mass is μ_η, whereas the charged scalars, in the basis $\Phi_+^T = (\eta_2^+, \eta_1^{-*})$, will have a mass matrix which is given below:

$$\mathcal{L} \ni -\Phi_+^\dagger \begin{pmatrix} \mu_\eta^2 + m_{\eta_2}^2 + \frac{g^2-g'^2}{4} v^2 \cos(2\beta) & b_\eta \\ b_\eta & \mu_\eta^2 + m_{\eta_1}^2 - \frac{g^2-g'^2}{4} v^2 \cos(2\beta) \end{pmatrix} \Phi_+. \tag{4}$$

Here, g, g' are the gauge couplings of $\mathrm{SU}(2)_L$ and $\mathrm{U}(1)_Y$, respectively. β is defined as $\tan\beta = \frac{v_2}{v_1} = \frac{\langle H_u^0 \rangle}{\langle H_d^0 \rangle}$ and $v^2 = v_1^2 + v_2^2$. We can diagonalize the above mass matrix by taking Φ_+ as

$$\Phi_+ = \begin{pmatrix} \cos\theta & -\sin\theta \\ \sin\theta & \cos\theta \end{pmatrix} \begin{pmatrix} \eta_{m2}^+ \\ \eta_{m1}^+ \end{pmatrix}, \qquad \tan 2\theta = \frac{2b_\eta}{m_{\eta_2}^2 - m_{\eta_1}^2 + (g^2 - g'^2)v^2\cos(2\beta)/2}. \tag{5}$$

Here, η_{m1}^+ and η_{m2}^+ are mass eigenstates of the charged scalar fields and we denote their mass eigenvalues by m_{1+} and m_{2+}, respectively.

The neutral fermionic and scalar components of $\hat{\eta}_1, \hat{\eta}_2, \hat{\chi}$ can be written as $\Psi^{\mathrm{T}} = (\tilde{\eta}_1^0, \tilde{\eta}_2^0, \tilde{\chi})$ and $\Phi_0^{\mathrm{T}} = (\eta_1^0, \eta_2^0, \chi)$, respectively. The neutral fermionic fields will have a mixing mass matrix, which is given below:

$$\mathcal{L} \ni -\frac{1}{2}\Psi^{\mathrm{T}} M_\eta \Psi, \qquad M_\eta = \begin{pmatrix} 0 & -\mu_\eta & -\lambda_2 v_2 \\ -\mu_\eta & 0 & \lambda_1 v_1 \\ -\lambda_2 v_2 & \lambda_1 v_1 & \mu_\chi \end{pmatrix}. \tag{6}$$

The above mixing matrix can be diagonalized by an orthogonal matrix as

$$U_\eta^{\mathrm{T}} M_\eta U_\eta = \mathrm{diag}(m_{\tilde{\eta}_1}, m_{\tilde{\eta}_2}, m_{\tilde{\eta}_3}). \tag{7}$$

The neutral scalar fields of Φ_0 can be written as

$$\Phi_0 = \frac{1}{\sqrt{2}}\Phi_R + \frac{i}{\sqrt{2}}\Phi_I = \frac{1}{\sqrt{2}} \begin{pmatrix} \eta_{1R}^0 \\ \eta_{2R}^0 \\ \chi_R \end{pmatrix} + \frac{i}{\sqrt{2}} \begin{pmatrix} \eta_{1I}^0 \\ \eta_{2I}^0 \\ \chi_I \end{pmatrix}. \tag{8}$$

The mixing matrix among these fields can be written as

$$\mathcal{L} \ni -\frac{1}{2}\Phi_R^{\mathrm{T}} m_{\eta_R}^2 \Phi_R - \frac{1}{2}\Phi_I^{\mathrm{T}} m_{\eta_I}^2 \Phi_I. \tag{9}$$

Here, the mixing matrices $m_{\eta_R}^2, m_{\eta_I}^2$ can be obtained from the following matrix:

$$\begin{aligned} m_\eta^2(\epsilon) &= \begin{pmatrix} m_{11}^2 & m_{12}^2 & m_{13}^2 \\ m_{12}^2 & m_{22}^2 & m_{23}^2 \\ m_{13}^2 & m_{23}^2 & m_{33}^2 \end{pmatrix}, \qquad m_{11}^2 = \mu_\eta^2 + m_{\eta_1}^2 + \lambda_2^2 v_2^2 + \frac{g^2 + g'^2}{4} v^2 \cos(2\beta), \\ m_{22}^2 &= \mu_\eta^2 + m_{\eta_2}^2 + \lambda_1^2 v_1^2 - \frac{g^2 + g'^2}{4} v^2 \cos(2\beta), \qquad m_{33}^2 = \mu_\chi^2 + m_\chi^2 + \lambda_1^2 v_1^2 + \lambda_2^2 v_2^2 + \epsilon b_\chi, \\ m_{12}^2 &= -\lambda_1 \lambda_2 v_1 v_2 - \epsilon b_\eta, \qquad m_{13}^2 = -\lambda_1 v_1 \mu_\eta - \lambda_2 v_2 \mu_\chi - \epsilon[(A\lambda)_2 v_2 - \mu\lambda_2 v_1], \\ m_{23}^2 &= \lambda_1 v_1 \mu_\chi + \lambda_2 v_2 \mu_\eta + \epsilon[(A\lambda)_1 v_1 - \mu\lambda_1 v_2]. \end{aligned} \tag{10}$$

Here, ϵ can take $+1$ or -1. We have $m_{\eta_R}^2 = m_\eta^2(+1)$ and $m_{\eta_I}^2 = m_\eta^2(-1)$. These two mixing mass matrices can be diagonalized by orthogonal matrices U_R and U_I, which are defined below:

$$\begin{aligned} U_R^{\mathrm{T}} m_{\eta_R}^2 U_R &= \mathrm{diag}(m_{\eta_{R1}}^2, m_{\eta_{R2}}^2, m_{\eta_{R3}}^2), \\ U_I^{\mathrm{T}} m_{\eta_I}^2 U_I &= \mathrm{diag}(m_{\eta_{I1}}^2, m_{\eta_{I2}}^2, m_{\eta_{I3}}^2). \end{aligned} \tag{11}$$

At last, the fermionic and scalar components of right-handed neutrino superfields, $\hat{N}_i$, can be denoted by N_i and $\tilde{N}_i$, respectively. The fermionic components have masses M_i. The scalar components can be decomposed into mass eigenstates as

$$\tilde{N}_i = \frac{1}{\sqrt{2}}(\tilde{N}_{Ri} + i\tilde{N}_{Ii}). \tag{12}$$

The masses squared of $\tilde{N}_{Ri}$ and $\tilde{N}_{Ii}$, respectively, are

$$\begin{aligned} m_{Ri}^2 &= M_i^2 + (m_N^2)_i + (b_M)_i, \\ m_{Ii}^2 &= M_i^2 + (m_N^2)_i - (b_M)_i. \end{aligned} \tag{13}$$

III. NEUTRINO MASSES AND LFV PROCESSES

As described before, in the model of Ref. [8] neutrinos are massless at tree level due to the presence of the discrete symmetry $Z_2 \times Z_2'$. However, in this model neutrinos acquire masses at the one-loop level, whose diagrams are shown in Fig. 1 [8]. After computing these one-loop diagrams, we find the following mass matrix for neutrinos:

$$(m_\nu)_{ij} = \sum_{k,l=1}^{3} \frac{(Y_\nu)_{ik}(Y_\nu)_{jk}}{16\pi^2} M_k \left[[U_R(2,l)]^2 \frac{m^2_{\eta_{Rl}}}{m^2_{\eta_{Rl}} - M_k^2} \ln \frac{m^2_{\eta_{Rl}}}{M_k^2} - [U_I(2,l)]^2 \frac{m^2_{\eta_{Il}}}{m^2_{\eta_{Il}} - M_k^2} \ln \frac{m^2_{\eta_{Il}}}{M_k^2} \right]$$
$$+ \sum_{k,l=1}^{3} \frac{(Y_\nu)_{ik}(Y_\nu)_{jk}}{16\pi^2} [U_\eta(2,l)]^2 m_{\tilde{\eta}_l} \left[\frac{m^2_{Rk}}{m^2_{Rk} - m^2_{\tilde{\eta}_l}} \ln \frac{m^2_{Rk}}{m^2_{\tilde{\eta}_l}} - \frac{m^2_{Ik}}{m^2_{Ik} - m^2_{\tilde{\eta}_l}} \ln \frac{m^2_{Ik}}{m^2_{\tilde{\eta}_l}} \right]. \quad (14)$$

It is to be noticed that the first and second lines of the above equation arise from the left- and right-hand diagrams of Fig. 1.

In our work we assume supersymmetry breaking to be around 1 TeV. Hence, we can take all the supersymmetric (SUSY) particle masses to be around a few hundred GeV. With this assumption, we can estimate the neutrino Yukawa couplings by requiring the neutrino mass scale to be around 0.1 eV [2]. With this requirement, we find that $(Y_\nu)_{ij} \sim 10^{-5}$. Here there are six different Yukawa couplings, which need to be suppressed to $\mathcal{O}(10^{-5})$. This could be one possibility in this model in order to explain the correct magnitude for neutrino masses. However, in this case, since the Yukawa couplings are suppressed, LFV processes such as $\ell_i \to \ell_j \gamma$ would also be suppressed. These LFV processes will be searched in future experiments [20], and hence it is worth considering the case where these processes can have a substantial contribution in this model. In other words, we have to look for a parameter region where we can have $(Y_\nu)_{ij} \sim \mathcal{O}(1)$.

From Eq. (14), it can observed that each diagram of Fig. 1 contributes positive and negative quantities to the neutrino mass matrix. Without suppressing Yukawa couplings, by fine-tuning the masses of SUSY particles we may achieve partial cancellation between the positive and negative contributions of Eq. (14) and end up with tiny masses for neutrinos. To demonstrate this explicitly, using Eq. (13) we can notice that in the limit $(b_M)_i \to 0$ we get $m^2_{Ri} - m^2_{Ii} \to 0$, and hence the second line of Eq. (14) would give a tiny contribution. The first line of Eq. (14) can give a very small value in the following limiting process: $U_R(2,l) - U_I(2,l) \to 0$ and $m_{\eta_{Rl}} - m_{\eta_{Il}} \to 0$. To achieve this limiting process we have to make sure that the elements of the matrices $m^2_{\eta_R}$ and $m^2_{\eta_I}$ are close to each other. From the discussion around Eq. (10), we can observe that the elements of $m^2_{\eta_R}$ and $m^2_{\eta_I}$ can differ by quantities which are proportional to ϵ. These quantities depend on the following parameters: b_χ, b_η, $(A\lambda)_1$, and $(A\lambda)_2$. By taking the limit $(A\lambda)_1 - \lambda_1\mu v_2/v_1 \to 0$, $(A\lambda)_2 - \lambda_2\mu v_1/v_2 \to 0$, $b_\eta \to 0$, $b_\chi \to 0$ we can get a tiny contribution from the first line of Eq. (14). To sum up the above discussion, without suppressing the neutrino Yukawa couplings we can fine-tune the following seven parameters, in order to get very small neutrino masses in this model:

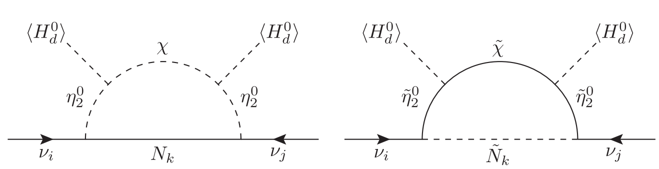

FIG. 1. Radiative masses for neutrinos.

$$(b_M)_i, i = 1,2,3, \qquad b_\eta, \qquad b_\chi, \qquad (A\lambda)_1, \qquad (A\lambda)_2. \quad (15)$$

Apparently, the above parameters are SUSY-breaking soft parameters of the scalar potential of this model. A study of neutrino masses depending on SUSY-breaking soft parameters can be seen in Ref. [21].

In the previous paragraph we have argued that Majorana masses for neutrinos are vanishingly small when we fine-tune certain soft parameters of the model. We can understand these features from symmetry arguments. For instance, when lepton number is conserved, neutrinos cannot have Majorana masses. For lepton number, we can propose a group $\mathrm{U}(1)_L$, under which the following fields are assigned the corresponding charges and the rest of the superfields are singlets:

$$\hat{L}_i \mapsto +1, \qquad \hat{E}_i^c \mapsto -1, \qquad \hat{N}_i \mapsto -1. \quad (16)$$

With the above-mentioned charges, we can see that the last terms in Eqs. (1) and (2) are forbidden. In fact, in the limit $M_i \to 0$ and $(b_M)_i \to 0$, the two diagrams of Fig. 1 give zero masses to neutrinos. Hence, in order to get Majorana masses for neutrinos, we have softly broken the lepton number symmetry. Now, even if we have $M_i \neq 0$, we have described in the previous paragraph that the left-hand diagram of Fig. 1 can still give vanishingly small masses by fine-tuning some soft parameters. This suggests that apart from $\mathrm{U}(1)_L$ there can exist some additional symmetries. Suppose we set $(A\lambda)_1 v_1 - \lambda_1 \mu v_2 = 0$, $(A\lambda)_2 v_2 - \lambda_2 \mu v_1 = 0$. Then (as argued previously) the left-hand diagram of Fig. 1 gives zero neutrino masses for $b_\eta \to 0$ and $b_\chi \to 0$, even if $M_i \neq 0$. This case can be understood by proposing an additional symmetry $U(1)_\eta$, under which the following fields have nontrivial charges and the rest of the fields are singlets:

$$\hat{L}_i \mapsto +1, \qquad \hat{E}_i^c \mapsto -1, \qquad \hat{\eta}_1 \mapsto -1,$$
$$\hat{\eta}_2 \mapsto -1, \qquad \hat{\chi} \mapsto +1. \tag{17}$$

Using the above charges, we can notice that μ_η and μ_χ terms in Eq. (1) and b_η and b_χ terms in Eq. (2) are forbidden. Thus, the additional symmetry $U(1)_\eta$ can forbid the Majorana masses for neutrinos in the left-hand diagram of Fig. 1. Finally, one may ask how the relations $(A\lambda)_1 v_1 - \lambda_1 \mu v_2 = 0$, $(A\lambda)_2 v_2 - \lambda_2 \mu v_1 = 0$ can be satisfied. In these two relations, SUSY-breaking soft masses are related to the SUSY-conserving mass μ. These relations may be achieved my proposing certain symmetries in the mechanism for SUSY breaking, which is beyond the reach of our present work.

Previously, we have motivated a parameter region where the neutrino Yukawa couplings can be $\mathcal{O}(1)$. For these values of the neutrino Yukawa couplings, LFV processes such as $\ell_i \to \ell_j \gamma$ can have substantial contributions in our model, and it is worth computing them. The Feynman diagrams for $\ell_i \to \ell_j \gamma$ are given in Fig. 2.

The general form of the amplitude for $\ell_i \to \ell_j \gamma$ is as follows:

$$\mathcal{M} = e\epsilon_\mu^*(q)\bar{u}_j(p-q)\left[A_L^{(ij)}\frac{1-\gamma_5}{2} + A_R^{(ij)}\frac{1+\gamma_5}{2}\right] \times i\sigma^{\mu\nu}q_\nu u_i(p). \tag{18}$$

It is to be noted that in the above equation, there is no summation over the indices i, j. The quantities $A_{L,R}^{(ij)}$ of the above equation can be found from the one-loop diagrams of Fig. 2, which we give below:

$$A_L^{(ij)} = A^{(ij)} m_j, \qquad A_R^{(ij)} = A^{(ij)} m_i,$$
$$A^{(ij)} = \sum_{k=1}^{3} \frac{(Y_\nu)_{ik}(Y_\nu)_{jk}}{16\pi^2}\left\{\frac{1}{4\mu_\eta^2}[f_2(x_{Rk}) + f_2(x_{Ik})] - \left[\cos^2\theta \frac{f_2(x_{k2})}{2m_{2+}^2} + \sin^2\theta \frac{f_2(x_{k1})}{2m_{1+}^2}\right]\right\},$$
$$x_{Rk} = \frac{m_{Rk}^2}{\mu_\eta^2}, \quad x_{Ik} = \frac{m_{Ik}^2}{\mu_\eta^2}, \quad x_{k2} = \frac{M_k^2}{m_{2+}^2}, \quad x_{k1} = \frac{M_k^2}{m_{1+}^2},$$
$$f_2(x) = \frac{1}{(1-x)^4}\left[\frac{1}{6} - x + \frac{1}{2}x^2 + \frac{1}{3}x^3 - x^2 \ln(x)\right]. \tag{19}$$

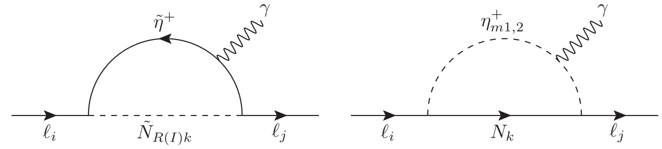

FIG. 2. Lepton-flavor-violating decays of the form $\ell_i \to \ell_j \gamma$.

From the above expressions, we can notice that in the curly brackets of $A^{(ij)}$, the first two and last two terms arise from the left- and right-hand diagrams of Fig. 2, respectively. Moreover, there is a relative minus sign in the contribution from these two diagrams.

Among the various decays of the form $\ell_i \to \ell_j \gamma$, the upper bound on the branching ratio of $\mu \to e\gamma$ is found to be stringent [5]. Moreover, we have $\mathrm{Br}(\mu \to e\bar{\nu}_e \nu_\mu) \approx 100\%$. Using this and neglecting the electron mass, the branching ratio of $\mu \to e\gamma$ is found to be

$$\mathrm{Br}(\mu \to e\gamma) = \frac{3\alpha}{16\pi G_F^2}\left|\sum_{k=1}^{3}(Y_\nu)_{1k}(Y_\nu)_{2k} \times \left\{\frac{1}{4\mu_\eta^2}[f_2(x_{Rk}) + f_2(x_{Ik})] - \left[\cos^2\theta \frac{f_2(x_{k2})}{2m_{2+}^2} + \sin^2\theta \frac{f_2(x_{k1})}{2m_{1+}^2}\right]\right\}\right|^2. \tag{20}$$

Here, $\alpha = \frac{e^2}{4\pi}$ and G_F is the Fermi constant.

Here we compare our work with that of Ref. [14]. The model in Ref. [14] is similar to that of Ref. [8]. But, in Ref. [14] a theory at a high scale with an anomalous $\mathrm{U}(1)_X$ symmetry was assumed. The $\mathrm{U}(1)_X$ symmetry breaks into Z_2 symmetry at a low scale. Due to these differences, there exist three one-loop diagrams for neutrinos in Ref. [14], whereas only two diagrams generate neutrino masses in Ref. [8]. The diagrams for the LFV processes of $\ell_i \to \ell_j \gamma$ in Ref. [14] are similar to the diagrams given in this paper (see Fig. 2). But the expression for $\mathrm{Br}(\mu \to e\gamma)$, which is given in Eq. (20), is found to be different from that in Ref. [14]. We hope that these differences might have arisen because the model in Ref. [14] has a different origin than that of Ref. [8].

Although the main motivation of this paper is to study the correlation between neutrino masses and $\mathrm{Br}(\mu \to e\gamma)$, below we mention muon $g-2$ in our model. It is known that the theoretical [22] and experimental [23] values of muon $g-2$ differ by about 3σ. However, there are hadronic uncertainties to muon $g-2$, which need to be improved [22]. Hence, the above-mentioned result is still an indication for a new physics signal. In our model [8], muon $g-2$ get contributions from MSSM fields [24] as well as from additional fields, which are shown in Table I. The contribution from MSSM fields can fit the 3σ discrepancy of muon $g-2$.[1] Hence, in our model [8], it is interesting to know how large the contribution from the additional fields of this model would be. The contribution from these additional fields can be found from the amplitude of Eq. (18), which is

$$\Delta a_\mu = \frac{m_\mu^2}{16\pi^2}\sum_{k=1}^{3}[(Y_\nu)_{2k}]^2\left\{\frac{1}{2\mu_\eta^2}[f_2(x_{Rk})+f_2(x_{Ik})] - \left[\cos^2\theta\frac{f_2(x_{k2})}{m_{2+}^2}+\sin^2\theta\frac{f_2(x_{k1})}{m_{1+}^2}\right]\right\}. \quad (21)$$

Here, m_μ is mass of the muon.

IV. ANALYSIS AND RESULTS

As described in Sec. I, our motivation is to study the correlation between neutrino masses and $\mathrm{Br}(\mu\to e\gamma)$. We have given the expression for neutrino masses in Eq. (14). We have explained in the previous section that to explain a neutrino mass scale of 0.1 eV, we can make the neutrino Yukawa couplings to be about $\mathcal{O}(1)$, but we need to fine-tune certain SUSY-breaking soft parameters which are given in Eq. (15). We consider this case, since for unsuppressed neutrino Yukawa couplings $\mathrm{Br}(\mu\to e\gamma)$ can have maximum values. As mentioned before, experiments have found the following upper bound: $\mathrm{Br}(\mu\to e\gamma) < 5.7\times10^{-13}$ [5]. Hence, for the above-mentioned parameter space, where neutrino Yukawa couplings are unsuppressed, we compute $\mathrm{Br}(\mu\to e\gamma)$ by fitting neutrino masses. We check if the computed values for $\mathrm{Br}(\mu\to e\gamma)$ satisfy the experimental bound [5].

Before we compute $\mathrm{Br}(\mu\to e\gamma)$, we first need to ensure that the neutrino Yukawa couplings can be unsuppressed in our model. We can calculate these Yukawa couplings from Eq. (14) by fitting to the neutrino oscillation data. The neutrino mass matrix of Eq. (14) is related to neutrino mass eigenvalues through the following relation:

$$m_\nu = U^*_{\mathrm{PMNS}}\mathrm{diag}(m_1,m_2,m_3)U^\dagger_{\mathrm{PMNS}}. \quad (22)$$

Here, $m_{1,2,3}$ are the mass eigenvalues of neutrinos and U_{PMNS} is the Pontecorvo-Maki-Nakagawa-Sakata matrix. The matrix U_{PMNS} depends on three mixing angles $(\theta_{12},\theta_{23},\theta_{13})$ and Dirac CP-violating phase, δ_{CP}. In the above equation there is a possibility of Majarona phases, which we have taken to be zero, for simplicity. We have parametrized U_{PMNS} in terms of mixing angles and δ_{CP} as it is given in Ref. [7].

By fitting to various neutrino oscillation data, we know solar and atmospheric neutrino mass-squared differences and also about the neutrino mixing angles [26]. In the case of normal hierarchy (NH) of neutrino masses, we have taken the mass-squared differences as

$$\Delta m_{21}^2 = m_2^2 - m_1^2 = 7.6\times10^{-5}\ \mathrm{eV}^2, \qquad |\Delta m_{31}^2| = |m_3^2 - m_1^2| = 2.48\times10^{-3}\ \mathrm{eV}^2. \quad (23)$$

In the case of inverted hierarchy (IH) of neutrino masses, the value of Δm_{21}^2 remains the same as mentioned above, but $|\Delta m_{31}^2| = 2.38\times10^{-3}\ \mathrm{eV}^2$. In this work, the neutrino mixing angles and CP-violating phase are chosen to be

$$\sin\theta_{12} = \frac{1}{\sqrt{3}}, \qquad \sin\theta_{23} = \frac{1}{\sqrt{2}}, \qquad \sin\theta_{13} = 0.15, \qquad \delta_{\mathrm{CP}} = 0. \quad (24)$$

The above-mentioned neutrino mass-squared differences, mixing angles, and the CP-violating phase are consistent with the fitted values in Ref. [26]. From the mass-squared differences, we can estimate neutrino mass eigenvalues which are given below for the cases of NH and IH, respectively:

$$m_1 = 0, \qquad m_2 = \sqrt{\Delta m_{21}^2}, \qquad m_3 = \sqrt{|\Delta m_{31}^2|}, \quad (25)$$

390

$$m_3 = 0, \qquad m_1 = \sqrt{|\Delta m_{31}^2|}, \qquad m_2 = \sqrt{\Delta m_{21}^2 + m_1^2}. \quad (26)$$

In the previous paragraph, we mentioned numerical values of neutrino mass eigenvalues, mixing angles, and the CP-violating phase. By plugging these values into Eq. (22), we can compute the elements of the matrix m_ν, which are related to neutrino Yukawa couplings and SUSY parameters through Eq. (14). Using Eq. (14), we can calculate the neutrino Yukawa couplings in order to satisfy neutrino oscillation data. This calculation procedure would be simplified if we assume degenerate masses for right-handed neutrinos and right-handed sneutrinos. For $i=1, 2, 3$, we assume the following:

$$M_i = M, \qquad (m_N^2)_i = m_N^2, \qquad (b_M)_i = b_M. \quad (27)$$

Under the above assumption, all three right-handed neutrinos have mass M. The corresponding sneutrinos have real and imaginary components [see Eq. (12)], whose masses would be

$$m_R^2 = M^2 + m_N^2 + b_M, \qquad m_I^2 = M^2 + m_N^2 - b_M. \quad (28)$$

Under the above-mentioned assumption, the neutrino mass matrix of Eq. (14) will be simplified to

[1] In Ref. [25], the discrepancy in muon $g-2$ was fitted in a supersymmetric model, where the contribution is actually from the MSSM fields.

$$(m_\nu)_{ij} = \frac{S_{ij}}{16\pi^2}\sum_{l=1}^{3}\left\{ M\left[[U_R(2,l)]^2 \frac{m^2_{\eta_{Rl}}}{m^2_{\eta_{Rl}} - M^2}\ln\frac{m^2_{\eta_{Rl}}}{M^2} - [U_I(2,l)]^2 \frac{m^2_{\eta_{Il}}}{m^2_{\eta_{Il}} - M^2}\ln\frac{m^2_{\eta_{Il}}}{M^2}\right] + [U_\eta(2,l)]^2 m_{\tilde{\eta}_l} \times \left[\frac{m^2_R}{m^2_R - m^2_{\tilde{\eta}_l}}\ln\frac{m^2_R}{m^2_{\tilde{\eta}_l}} - \frac{m^2_I}{m^2_I - m^2_{\tilde{\eta}_l}}\ln\frac{m^2_I}{m^2_{\tilde{\eta}_l}}\right]\right\}, \quad (29)$$

$$S_{ij} = \sum_{k=1}^{3}(Y_\nu)_{ik}(Y_\nu)_{jk}. \quad (30)$$

The elements S_{ij} are quadratic in the neutrino Yukawa couplings. From the above relation we can see that for certain values of the SUSY parameters, S_{ij} can be calculated from $(m_\nu)_{ij}$. Using the above-mentioned assumption of degenerate masses for right-handed neutrinos and right-handed sneutrinos, we can see that Eqs. (20) and (21) would give us $\mathrm{Br}(\mu \to e\gamma) \propto S^2_{21}$ and $\Delta a_\mu \propto S_{22}$.

In our model, there are plenty of SUSY parameters, and we need to fix some of them to simplify our analysis. In our analysis, we choose the following SUSY parameters:

$$\mu_\chi = 600\ \mathrm{GeV}, \quad m_{\eta_1} = 400\ \mathrm{GeV}, \quad m_{\eta_2} = 500\ \mathrm{GeV}, \quad m_\chi = 600\ \mathrm{GeV}, \quad m_N = 700\ \mathrm{GeV}, \quad \lambda_1 = 0.5, \quad \lambda_2 = 0.6, \quad \tan\beta = 10. \quad (31)$$

We freely vary the parameters μ_η and M. In the previous section, we explained that we need to fine-tune the parameters of Eq. (15) in order to get small neutrino masses. Among these parameters, we take $(A\lambda)_1 = \lambda_1\mu v_2/v_1$ and $(A\lambda)_2 = \lambda_2\mu v_1/v_2$. The other parameters of Eq. (15), without loss of generality, are taken to be degenerate:

$$b_M = b_\eta = b_\chi = b_{\mathrm{susy}}. \quad (32)$$

We have explained before that we have assumed degenerate masses for right-handed neutrinos and right-handed sneutrinos. Under this assumption, information about the neutrino Yukawa couplings is contained in the quantities S_{ij}. Hence, it is worth plotting these quantities to understand the neutrino Yukawa couplings. In Fig. 3, for the case of NH, we plot S_{21} and S_{22} versus the right-handed neutrino mass M for $\mu_\eta = 1$ TeV. The plots of Fig. 3 indicate that S_{22} and S_{21} are around $\mathcal{O}(1)$. Since these quantities are the sum of the squares of neutrino Yukawa couplings [see Eq. (30)], we can expect that the neutrino Yukawa couplings should be in the range of $\mathcal{O}(1)$. We do not plot the values of S_{11}, S_{31}, etc. in Fig. 3, but we have found that these will also be around $\mathcal{O}(1)$. We plot S_{21} and S_{22} in Fig. 3, since these two determine $\mathrm{Br}(\mu \to e\gamma)$ and Δa_μ.

From the plots of Fig. 3, we can notice that the values of S_{22} are higher than those of S_{21}. This fact follows from Eq. (29), where we can see that S_{ij} are proportional to $(m_\nu)_{ij}$, which are determined by neutrino oscillation parameters. In the case of NH, we have seen that $(m_\nu)_{22}$ is greater than $(m_\nu)_{21}$ by a factor of 3.4, and hence S_{22} is always found to be larger than S_{21}. It is clear from the plots of Fig. 3 that by increasing b_{susy}, S_{21} and S_{22} would decrease. Again, this feature can be understood from Eq. (29). As explained in the previous section, the square brackets of Eq. (29) would tend to zero in the limit $b_{\mathrm{susy}} \to 0$. So for a large value of b_{susy} there will be less partial cancellation in the square brackets, and hence S_{21} and S_{22} would decrease. In both plots of Fig. 3 it is found that the values of S_{21} and S_{22} initially decrease with M, go to a minima, and then increase. The shape of these

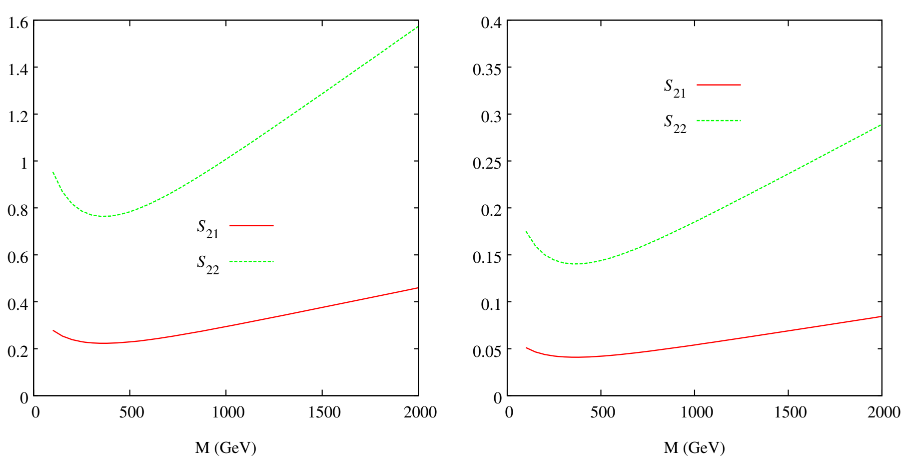

FIG. 3 (color online). The quantities S_{21}, S_{22} are plotted against the right-handed neutrino mass for $\mu_\eta = 1$ TeV, in the case of NH. In the left- and right-hand plots, b_{susy} is taken to be $(3 \times 10^{-2})^2$ GeV^2 and $(7 \times 10^{-2})^2$ GeV^2, respectively.

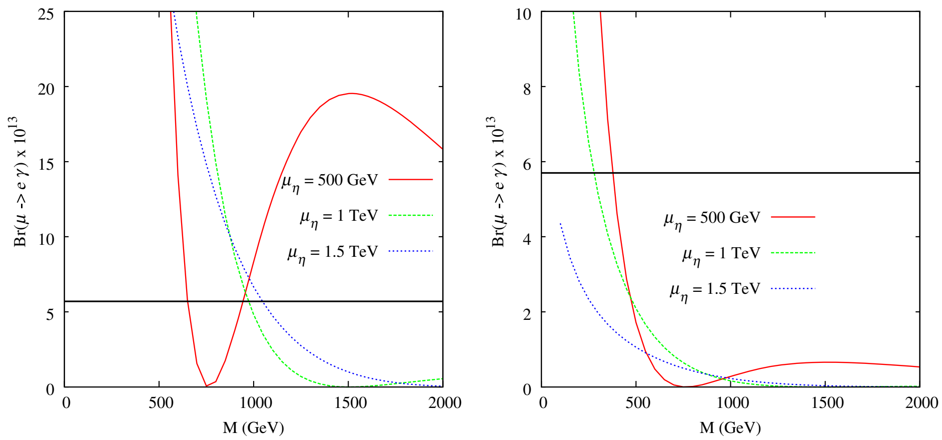

FIG. 4 (color online). $\mathrm{Br}(\mu \to e\gamma)$ is plotted against the right-handed neutrino mass for different values of μ_η. In the left- and right-hand plots, b_{susy} is taken as $(3 \times 10^{-2})^2\ \mathrm{GeV}^2$ and $(7 \times 10^{-2})^2\ \mathrm{GeV}^2$, respectively. The horizontal line indicates the current upper bound on $\mathrm{Br}(\mu \to e\gamma)$.

curves can be understood by applying the approximation of $\frac{b_{\mathrm{susy}}}{M^2} \ll 1$ in Eq. (29). In the limit $b_{\mathrm{susy}} \to 0$, we can take

$$m^2_{\eta_{Rl}} = m^2_{\eta_l}(1 + \delta_{Rl}), \qquad m^2_{\eta_{Il}} = m^2_{\eta_l}(1 + \delta_{Il}),$$
$$U_R(2, l) \approx U_I(2, l) = U_0(2, l). \tag{33}$$

Here, $\delta_{Rl}, \delta_{Il} \ll 1$. Using the above-mentioned approximations in Eq. (29), we get

$$\begin{aligned}(m_\nu)_{ij} = \frac{S_{ij}}{16\pi^2} \sum_{l=1}^{3} \Bigg\{ &[U_0(2, l)]^2 (\delta_{Rl} - \delta_{Il}) M \frac{m^2_{\eta_l}}{m^2_{\eta_l} - M^2} \\ &\times \left[1 - \frac{M^2}{m^2_{\eta_l} - M^2} \ln \frac{m^2_{\eta_l}}{M^2}\right] \\ &+ [U_\eta(2, l)]^2 m_{\tilde{\eta}_l} \frac{2b_{\mathrm{susy}}}{M^2 + m_N^2 - m^2_{\tilde{\eta}_l}} \\ &\times \left[1 - \frac{m^2_{\tilde{\eta}_l}}{M^2 + m_N^2 - m^2_{\tilde{\eta}_l}} \ln \frac{M^2 + m_N^2}{m^2_{\tilde{\eta}_l}}\right] \Bigg\}. \end{aligned} \tag{34}$$

In the summation of the above equation, the first and second lines arise due to the left- and right-hand diagrams of Fig. 1. From the above equation, we can understand that the contribution from the first line increases, reaches a maximum, and then decreases with M, whereas, the contribution from the second line of the above equation decreases monotonically with M. It is this functional dependence on M that determines the shape of the lines in Fig. 3. Physically, in the limit $b_{\mathrm{susy}} \to 0$, the above description suggests that the right-hand diagram of Fig. 1 is significant only for very low values of M. For other values of M, the left-hand diagram of Fig. 1 gives the dominant contribution to neutrino masses. One remark about the plots in Fig. 3 is that we have fixed $\mu_\eta = 1$ TeV in these figures. We have varied μ_η from 500 GeV to 1.5 TeV and have found that the plots in Fig. 3 would change quantitatively, but qualitative features would remain same. Also, the plots in Fig. 3 are for the case of NH. Again, these plots can change quantitatively, if not qualitatively, for the case of IH. For this reason, below we present our results on $\mathrm{Br}(\mu \to e\gamma)$ and muon $g - 2$ for the case of NH only.

As described before, our motivation is to compute $\mathrm{Br}(\mu \to e\gamma)$ in the model of Ref. [8]. In Fig. 3 we show that the neutrino Yukawa couplings in this model can be $\mathcal{O}(1)$, and for these values of Yukawa couplings $\mathrm{Br}(\mu \to e\gamma)$ is unsuppressed. In the parameter space where the neutrino Yukawa couplings are unsuppressed, we plot $\mathrm{Br}(\mu \to e\gamma)$ as a function of the right-handed neutrino mass. These plots are shown in Fig. 4, where we also vary μ_η from 500 GeV to 1.5 TeV. The horizontal line in these plots indicates the current upper bound of $\mathrm{Br}(\mu \to e\gamma) < 5.7 \times 10^{-13}$. This upper bound would impose a lower bound on the right-handed neutrino mass, as can be seen in the plots of Fig. 4. In the left-hand plot of Fig. 4, for $\mu_\eta = 500$ GeV, the right-handed neutrino mass is allowed to be between about 650 to 950 GeV. In the same plot, for $\mu_\eta = 1$ or 1.5 TeV, the right-handed neutrino mass has a lower bound of about 1 TeV. In the right-hand plot of Fig. 4, the lower bound on the right-handed neutrino mass is within 500 GeV, even for a low value of $\mu_\eta = 500$ GeV.

The lower bounds on the right-handed neutrino mass M are severe in the left-hand plot of Fig. 4. The reason is that for a low value of b_{susy}, S_{21} would be high, and hence $\mathrm{Br}(\mu \to e\gamma)$ would be large. From Fig. 4, we can observe that $\mathrm{Br}(\mu \to e\gamma)$ initially decreases with M, goes to a minimum, and then increases. For instance, in the left-hand plot of Fig. 4, for $\mu_\eta = 500$ GeV, $\mathrm{Br}(\mu \to e\gamma)$ goes to a minimum around $M = 750$ GeV, and then it has a local maxima around $M = 1.5$ TeV. The reason that $\mathrm{Br}(\mu \to e\gamma)$ initially decreases with M is due to the fact that the decay $\mu \to e\gamma$ is driven by right-handed neutrinos and right-handed sneutrinos, as given in Fig. 2. The masses of right-handed neutrinos and right-handed sneutrinos are proportional to M, and hence $\mathrm{Br}(\mu \to e\gamma)$ would be suppressed with increasing M. After that, at a certain value of M, $\mathrm{Br}(\mu \to e\gamma)$ would tend to become zero. The reason for this is that the sum of the two diagrams of Fig. 2 gives a relative minus sign to the contribution of $\mathrm{Br}(\mu \to e\gamma)$, which is given in Eq. (20). Hence, for a particular value of

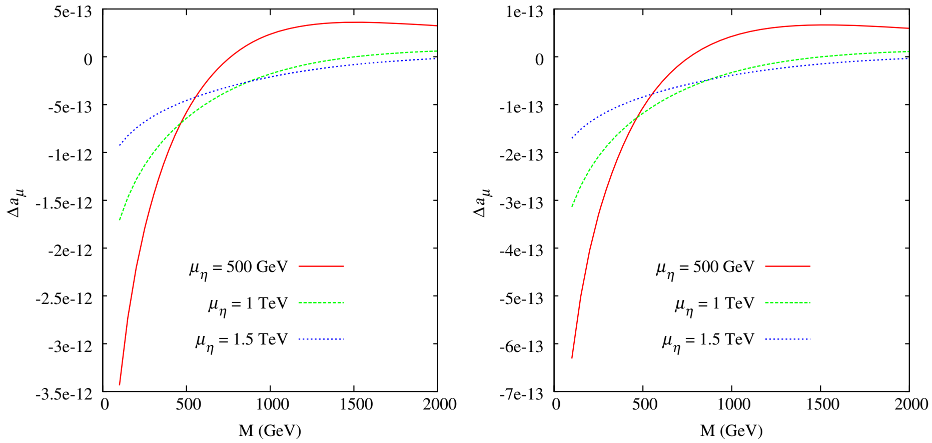

FIG. 5 (color online). Δa_μ is plotted against the right-handed neutrino mass for different values of μ_η. In the left- and right-hand plots, b_{susy} is taken as $(3\times10^{-2})^2$ GeV^2 and $(7\times10^{-2})^2$ GeV^2, respectively.

M, the contributions from both diagrams of Fig. 2 cancel out and give a minimum for $\mathrm{Br}(\mu\to e\gamma)$. Also, $\mathrm{Br}(\mu\to e\gamma)$ can go to zero asymptotically when $M\to\infty$, since in this limit the masses of right-handed neutrinos and right-handed sneutrinos would become infinitely large and suppress $\mathrm{Br}(\mu\to e\gamma)$. Hence, $\mathrm{Br}(\mu\to e\gamma)$ has two zeros on the M axis. As $\mathrm{Br}(\mu\to e\gamma)$ is a continuous function of M and is always a positive quantity, it has a local maxima between the two zeros on the M axis.

In the previous section we described muon $g-2$. In Eq. (21), we have given the contribution due to additional fields (see Table I) of our model to the muon $g-2$. Apart from this contribution, the MSSM fields of our model also contribute to muon $g-2$ [24], and it is known that this contribution fits the 3σ discrepancy of muon $g-2$. Hence, it is interesting to know if the additional contribution of Eq. (21) could be as large as that of the MSSM contribution to muon $g-2$. In Fig. 5, we plot the contribution of Eq. (21). In the plots of Fig. 5, we have chosen the parameter region such that the neutrino oscillation data is fitted. From the plots of Fig. 5, we can see that for low values of M, Δa_μ can be negative and it becomes positive after a certain large value of M. From these plots we can notice that the overall magnitude of Δa_μ is not more than about 10^{-12}. This contribution is at least 2 orders of magnitude smaller than the estimated discrepancy of muon $g-2$, which is $(29\pm9)\times10^{-10}$ [22]. From this we can conclude that the additional contribution to muon $g-2$ in our model [i.e., Eq. (21)] is insignificant compared to the MSSM contribution to muon $g-2$.

V. CONCLUSIONS

We have worked in a supersymmetric model where neutrino masses arise at the one-loop level [8]. We have computed these loop diagrams and obtained expressions for neutrino masses. We have identified a parameter region of this model, where the neutrino oscillation data can be fitted without the need for suppressing the neutrino Yukawa couplings. In our parameter region, the SUSY-breaking soft parameters [such as b_M, b_η, b_χ, $(A\lambda)_1$, and $(A\lambda)_2$] need to be fine-tuned. In this parameter region, the branching fraction of $\mu\to e\gamma$ can be unsuppressed, and hence we have computed $\mathrm{Br}(\mu\to e\gamma)$. We have shown that the current upper bound on $\mathrm{Br}(\mu\to e\gamma)$ can put lower bounds on the mass of the right-handed neutrino field. Depending on the parametric choice, we have found that this lower bound can be about 1 TeV. We have also computed the contribution to muon $g-2$ arising from additional fields of this model, which are given in Table I. We have shown that, in the region where neutrino oscillation data is fitted, the above-mentioned contribution is 2 orders smaller than the discrepancy in muon $g-2$.

[1] C. Quigg, arXiv:hep-ph/0404228; J. Ellis, Nucl. Phys. **A827**, 187C (2009).

[2] R. N. Mohapatra, arXiv:hep-ph/0211252; Y. Grossman, arXiv:hep-ph/0305245; A. Strumia and F. Vissani, arXiv:hep-ph/0606054.

[3] H. P. Nilles, Phys. Rep. **110**, 1 (1984); H. E. Haber and G. L. Kane, Phys. Rep. **117**, 75 (1985); S. P. Martin, arXiv:hep-ph/9709356; M. Drees, R. Godbole, and P. Roy, *Theory and Phenomenology of Sparticles* (World Scientific, Singapore, 2004); P. Binetruy, *Supersymmetry* (Oxford University, New York, 2006); H. Baer and X. Tata, *Weak Scale Supersymmetry: From Superfields to Scattering Events* (Cambridge University Press, Cambridge, England, 2006).

[4] T. Mori, Proceedings of the Fourth International Conference on Flavor Physics and CP Violation in Vancouver, British Columbia, Canada, eConf C060409, 034 (2006); J. M. Yang, Int. J. Mod. Phys. A **23**, 3343 (2008); A. J. Buras, Acta Phys. Pol. B Proc. Suppl. **3**, 7 (2010); Y. Nir, CERN Yellow Report No. CERN-2010-001, 279 (2010).

[5] J. Adam *et al.* (MEG Collaboration), Phys. Rev. Lett. **110**, 201801 (2013).

[6] B. Aubert *et al.* (*BABAR* Collaboration), Phys. Rev. Lett. **104**, 021802 (2010).

[7] K. A. Olive *et al.* (Particle Data Group), Chin. Phys. C **38**, 090001 (2014).

[8] E. Ma, Annales Fond. Broglie **31**, 285 (2006).

[9] E. Ma, Phys. Rev. D **73**, 077301 (2006).

[10] R. Barbieri, L. J. Hall, and V. S. Rychkov, Phys. Rev. D **74**, 015007 (2006).

[11] A. Arhrib, R. Benbrik, J. E. Falaki, and A. Jueid, J. High Energy Phys. 12 (2015) 007; A. D. Plascencia, J. High Energy Phys. 09 (2015) 026; S. Kashiwase and D. Suematsu, Phys. Lett. B **749**, 603 (2015).

[12] Q.-H. Cao, E. Ma, J. Wudka, and C.-P. Yuan, arXiv:0711.3881.

[13] H. Fukuoka, J. Kubo, and D. Suematsu, Phys. Lett. B **678**, 401 (2009); D. Suematsu, T. Toma, and T. Yoshida, Int. J. Mod. Phys. A **25**, 4033 (2010).

[14] D. Suematsu and T. Toma, Nucl. Phys. **B847**, 567 (2011).

[15] E. Ma, Phys. Lett. B **659**, 885 (2008).

[16] E. Ma, Mod. Phys. Lett. A **23**, 721 (2008).

[17] I.-H. Lee, Phys. Lett. B **138**, 121 (1984); Nucl. Phys. **B246**, 120 (1984).

[18] U. Bellgardt *et al.* (SINDRUM Collaboration), Nucl. Phys. **B299**, 1 (1988).

[19] M. Aoki, J. Kubo, T. Okawa, and H. Takano, Phys. Lett. B **707**, 107 (2012).

[20] A. M. Baldini *et al.*, arXiv:1301.7225; T. Aushev *et al.*, arXiv:1002.5012.

[21] A. J. R. Figueiredo, Eur. Phys. J. C **75**, 99 (2015).

[22] F. Jegerlehner and A. Nyffeler, Phys. Rep. **477**, 1 (2009); T. Blum, A. Denig, I. Logashenko, E. de Rafael, B. Lee Roberts, T. Teubner, and G. Venanzoni, arXiv:1311.2198.

[23] G. W. Bennett *et al.* (Muon g-2 Collaboration), Phys. Rev. D **73**, 072003 (2006).

[24] T. Moroi, Phys. Rev. D **53**, 6565 (1996); **56**, 4424(E) (1997); S. P. Martin and J. D. Wells, Phys. Rev. D **64**, 035003 (2001).

[25] R. S. Hundi, Phys. Rev. D **83**, 115019 (2011).

[26] D. V. Forero, M. Tortola, and J. W. F. Valle, Phys. Rev. D **90**, 093006 (2014).